

PAPER • OPEN ACCESS

## Daily carbon dioxide fluxes in Arctic tundra and forest-tundra ecosystems in response to temperature and precipitation extremes

To cite this article: Elizaveta Gorbarenko *et al* 2025 *Environ. Res. Commun.* 7 055022

View the [article online](#) for updates and enhancements.

### You may also like

- [Tundra plant above-ground biomass and shrub dominance mapped across the North Slope of Alaska](#)  
Logan T Berner, Patrick Jantz, Ken D Tape *et al.*
- [The carbon sink due to shrub growth on Arctic tundra: a case study in a carbon-poor soil in eastern Canada](#)  
Mikael Gagnon, Florent Domine and Stéphane Boudreau
- [Water track distribution and effects on carbon dioxide flux in an eastern Siberian upland tundra landscape](#)  
Salvatore R Curasi, Michael M Loranty and Susan M Natali



www.hidenanalytical.com  
info@hiden.co.uk

# HIDEN ANALYTICAL

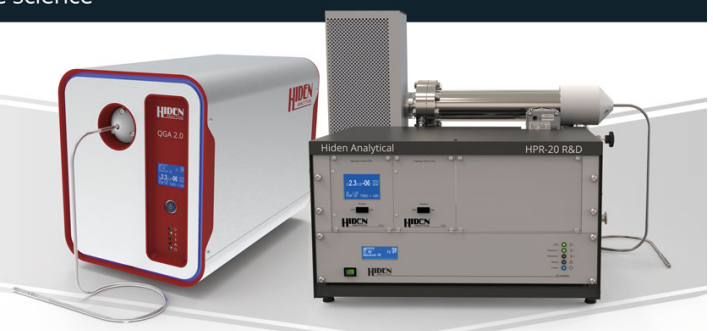
## Instruments for Advanced Science

Mass spectrometers for vacuum, gas, plasma and surface science



### Dissolved Species Analysis

Hiden offers MIMS capabilities in the form of a benchtop HPR-40 DSA system for laboratory-based research and the portable case mounted pQA for applications that favour in-situ measurements in the field. Both are supplied with a choice of membrane material and user-changeable sample inlets.



### Gas Analysis

The QGA and HPR-20 series gas analysers are versatile tools designed for a broad spectrum of environmental applications, including pollution monitoring, biogas analysis, and sustainable energy research.

## Environmental Research Communications



## PAPER

## Daily carbon dioxide fluxes in Arctic tundra and forest-tundra ecosystems in response to temperature and precipitation extremes

## OPEN ACCESS

RECEIVED  
30 October 2024REVISED  
19 February 2025ACCEPTED FOR PUBLICATION  
13 May 2025PUBLISHED  
23 May 2025

Original content from this work may be used under the terms of the [Creative Commons Attribution 4.0 licence](#).

Any further distribution of this work must maintain attribution to the author(s) and the title of the work, journal citation and DOI.

Elizaveta Gorbarenko<sup>1,2</sup> , Daria Gushchina<sup>1</sup> , Maria Tarasova<sup>1</sup> , Irina Zheleznova<sup>1</sup> , Ekaterina Emelianova<sup>2</sup>, Ravil Gibadullin<sup>1</sup> , Alexander Osipov<sup>1</sup> and Alexander Olchev<sup>1</sup> <sup>1</sup> Department of Meteorology and Climatology, Faculty of Geography, Lomonosov Moscow State University, GSP-1, Leninskie Gory, 1, 119991, Moscow, Russia<sup>2</sup> A.N. Severtsov Institute of Ecology and Evolution, Russian Academy of Science, Leninsky Prospekt 33, Moscow 119071, RussiaE-mail: [aoltche@yandex.ru](mailto:aoltche@yandex.ru)

**Keywords:** temperature and precipitation extremes, carbon dioxide fluxes, Arctic tundra and forest tundra, FLUXNET, reanalysis  
Supplementary material for this article is available [online](#)

**Abstract**

The development and functioning of landscapes in different regions of the world, especially at polar latitudes, may be significantly affected by the increased frequency of extreme weather events associated with modern climate change. These events can influence regional biogeochemical cycles, including water, carbon, and nitrogen cycles, with serious implications for ecosystem functioning and canopy production. The main objective of this study is to assess the spatial variability in the response of daily net ecosystem CO<sub>2</sub> exchange (NEE) of Northern Hemisphere tundra and forest-tundra landscapes to anomalous temperature and precipitation events during the growing season. These landscape types are considered to be among the most vulnerable to changes in environmental conditions under a changing climate. For our data analysis, we use meteorological and CO<sub>2</sub> flux data from the global FLUXNET and regional AmeriFlux networks, as well as the ERA5 reanalysis dataset. Analysis of CO<sub>2</sub> flux anomalies in tundra and forest-tundra ecosystems revealed a wide range of observed NEE responses to anomalous temperature and precipitation events during the growing season, depending on geographic location and landscape type. In contrast to most previous studies, the stressed CO<sub>2</sub> uptake and higher CO<sub>2</sub> emissions under anomalously high temperatures were mostly detected at the southern boundary of the polar region, where heat waves are more frequent. Prevailing CO<sub>2</sub> uptake during anomalously high temperature days was found in deciduous broadleaf forests and open shrublands. The effect of anomalously low temperature is manifested by an increase in CO<sub>2</sub> emissions. The response of CO<sub>2</sub> fluxes to anomalously high and low precipitation is quite similar regardless of the time scale (short-term or long-term response). In most tundra and forest-tundra ecosystems, heavy precipitation typically results in increased CO<sub>2</sub> emissions to the atmosphere. The prolonged precipitation deficit is accompanied by a prevailing CO<sub>2</sub> uptake.

**1. Introduction**

Arctic tundra and forest-tundra landscapes cover large continental areas in the Northern Hemisphere and provide a wide range of ecosystem services, including carbon sequestration, climate regulation, and biodiversity (Chapin *et al* 2005). Their essential role in the global carbon cycle is due to their significant soil carbon pool, accounting for about 30% of global soil carbon (Post *et al* 1982, Serreze *et al* 2000, Scharlemann *et al* 2014, Friedlingstein *et al* 2023).

Global warming, caused primarily by increasing concentrations of greenhouse gases (GHGs) in the Earth's atmosphere, is having a significant impact on ecosystems around the world (IPCC 2022). Particularly high rates of global warming are being observed in the polar latitudes of the Northern Hemisphere. The rate of temperature increase in the polar regions is, on average, about twice as high as the rate of temperature increase

for the entire globe (Post *et al* 2019, Rantanen *et al* 2022). This is likely to lead to significant changes in regional biogeochemical cycles, including water, carbon and nitrogen balances, with serious implications for ecosystem functioning and global climate feedbacks (Johannessen *et al* 2004, Francis *et al* 2017). Rising temperatures at polar latitudes may also lead to an increase in the Gross Primary Production (GPP) of the vegetation cover. Longer growing seasons, the northward expansion of woody and shrub vegetation due to increased nitrogen mineralization rates, and enhanced soil fertility may lead to an increase in soil carbon stocks (Davis and Gedalof 2018). At the same time, it should be taken into account that elevated temperature can lead to an increase in the rate of decomposition of organic matter, which in turn can result in an increase in the rate of soil respiration. At the current rate of global warming, more Arctic regions are gradually becoming a net source of CO<sub>2</sub> to the atmosphere (Oechel *et al* 1993, Schuur *et al* 2022). One of the major consequences of rapid temperature rise at polar latitudes is the thawing of permafrost, which leads to the release of large amounts of carbon dioxide (CO<sub>2</sub>) and methane (CH<sub>4</sub>) from previously frozen organic matter into the atmosphere. According to Natali *et al* (2019), under the RCP 8.5 climate change scenario, permafrost regions could release up to 200 billion tons of carbon into the atmosphere by 2100.

The observed rise in air temperatures is accompanied by an increase in the frequency and severity of extreme weather events in many regions of the world (Dobricic *et al* 2020, Bolan *et al* 2024). The polar latitudes are characterized by one of the highest rates of increase in the intensity and duration of positive temperature anomalies (Dobricic *et al* 2020, Rantanen *et al* 2024). Rantanen *et al* (2024) used atmospheric reanalysis and global climate models to show that the total area affected by severe heat waves in the Arctic has doubled, the area of extreme heat waves has tripled, and the area of very extreme heat waves has quadrupled since the mid-20th century. At polar latitudes, such extreme weather events can alter the structure and species composition of plant communities, disturbing plant functioning and leading to a reduction in biodiversity (Bokhorst *et al* 2022, Robinson 2022). Anomalously high temperatures in polar regions can lead to more intensive degradation of permafrost and increased emissions of CO<sub>2</sub> and CH<sub>4</sub> into the atmosphere (Schuur *et al* 2015, 2022). Dobricic *et al* (2020) hypothesize that the negative effects of the Arctic heat wave will be more severe, while polar plants and soil biota are adapted to temperatures that rise above freezing only for relatively short periods. Active reproduction of soil microorganisms begins at temperatures above 0 °C (Schuur *et al* 2015), and these processes can be particularly active during periods of unusually high temperatures for several consecutive days. As a result, particularly prolonged heat waves may increase the rate of decomposition of carbon stored in permafrost, leading to increased soil emissions of CO<sub>2</sub> and CH<sub>4</sub> into the atmosphere.

The effect of positive temperature anomalies on natural ecosystems at polar latitudes can vary in different seasons depending on the availability of snow cover, depth of permafrost, and species composition of woody, shrub, and herbaceous vegetation. Extreme short-term winter warming in the Arctic leads to rapid snowmelt, exposing ecosystems to unseasonably warm environmental conditions (Bokhorst *et al* 2011). When cold weather returns, vegetation may be exposed to much colder temperatures, in part due to reduced snowpack height, which has an insulating effect. As a result, short-term winter thaws can reduce plant reproduction and increase shoot mortality, leading to GPP reduction in the summer months. Rapid spring snowmelt due to anomalous temperature increases can lead to faster snowmelt, increased surface runoff, and enhanced evapotranspiration. Water from spring snowmelt infiltrates the soil and triggers fresh CO<sub>2</sub> production at higher rates (Arndt *et al* 2020). Flux measurements during the anomalously warm winter-spring conditions in Alaska and northwestern Canada showed that the extremely warm spring enhanced photosynthesis more than respiration, leading to greater CO<sub>2</sub> uptake in tundra ecosystems (Liu *et al* 2020). Similar results were obtained by Kwon *et al* (2021) for northern Siberia.

Prolonged and short-term warming during the growing season can lead to a variety of ecosystem responses and changes in CO<sub>2</sub> fluxes that are closely linked to local landscape conditions (Treharne *et al* 2020, Braybrook *et al* 2021, Maes *et al* 2024, Torn *et al* 2025). Mertens *et al* (2001), using data from chamber measurements at a tundra site in North and East Greenland, reported increased soil CO<sub>2</sub> fluxes mainly due to changes in plant and microbial respiration. Sufficient soil moisture availability favored insignificant changes in GPP. Zona *et al* (2014) analyzed eddy covariance data of CO<sub>2</sub> fluxes during the unusually hot summer of 2007 in Barrow, Arctic Alaska, and showed that despite significant *Sphagnum* moss desiccation, these abnormal conditions did not affect NEE from this wet-sedge Arctic tundra ecosystem. GPP and ecosystem respiration (RE) rates were generally higher during this extreme summer than in previous years. The authors note that the following year, after an unusually warm and dry summer, there were anomalously low rates of ecosystem CO<sub>2</sub> uptake despite relatively favorable environmental conditions. Importantly, the return to a substantial cumulative CO<sub>2</sub> sink occurred two summers after the extreme event, suggesting substantial resilience of this tundra ecosystem to at least one isolated extreme event.

Unusual drops in temperature can also have a significant impact on plant health and function. Late spring and early fall frosts are particularly dangerous, causing the most damage to active plant tissues that have not had

time to harden to withstand the cold (Pearce 2001, Zohner *et al* 2020). Summer frosts are also hazardous to plants and may lead to reduction of GPP rate (Bjerke *et al* 2014).

The study of the effects of abundant and scarce precipitation on the ecosystems of the polar latitudes is an equally important task in modern climate research, since the various ecosystems of this region are extremely sensitive to changes in the precipitation conditions (Zona *et al* 2014). The effects of extreme precipitation or prolonged dry spells in polar latitudes are most pronounced during warm periods. Heavy precipitation in tundra landscapes after prolonged soil drying can lead to anomalous pulsed CO<sub>2</sub> release from the soil (the so-called 'Birch' effect). This effect can vary in different ecosystems depending on vegetation structure, soil type and microbial community dynamics (Jarvis *et al* 2007). According to a study by Panov *et al* (2024) in the southern part of the Taimyr Peninsula, Siberia, an average additive effect of precipitation on soil CO<sub>2</sub> flux can reach 7%–12% over the entire growing season. A study by Bjerke *et al* (2014) showed that summer droughts in the Arctic can lead to widespread mortality of herbaceous plants, with particular effects on moss and lichen communities, and strong reductions in ecosystem GPP. Such a process may also lead to increased wildfire risk, which could completely destroy significant areas in tundra and forest-tundra landscapes (Berner *et al* 2012, Dvornikov *et al* 2022). On the other hand, unusually high and prolonged precipitation can cause a rise in groundwater levels, flooding of depressions and a decrease in GPP of vegetation due to reduced oxygen in the root zone of plants (Ohta *et al* 2014, Li *et al* 2022). In addition, unusually heavy precipitation leads to accelerated melting of permafrost, which in turn contributes to the release of old carbon and increased soil emissions of CO<sub>2</sub> and CH<sub>4</sub> into the atmosphere (Schoor *et al* 2015).

Despite the high risk of vulnerability of polar ecosystems due to the increasing frequency of extreme weather events, some polar ecosystems show high resilience and adaptation to external impacts. In particular, studies by Hollister *et al* (2005) have shown that some polar plant species are able to adapt to changes in temperature and precipitation conditions over time. However, the present rate of climate change may exceed the adaptive capacity of many plant species and ecosystems. The cumulative effects of recurrent extreme weather events may also damage polar ecosystems, leading to long-term changes. A study by Post *et al* (2009) has shown that recent climate changes associated with an increased frequency of extreme events have the potential to affect ecosystem services related to natural resources, plant functions, nutrient cycling, and carbon sequestration.

Thus, extreme weather events in the polar latitudes have profound and diverse effects on the state and functions of polar ecosystems. Changes in the dynamics and amplitude of photosynthetic processes in green plants and the intensity of ecosystem respiration are considered key indicators of the vital status of terrestrial ecosystems. As shown above, many studies have been conducted in recent decades to assess the impact of temperature rise and increased anomalous weather events (primarily anomalously high temperatures and droughts) on GHG emissions and uptake by natural ecosystems in the Arctic. Most studies have focused on analyzing changes in GHG fluxes due to global warming. Fewer studies have focused on assessing the short- and long-term effects of anomalous temperature events on GHG fluxes, with an emphasis on studying individual ecosystems (or several ecosystems within the same region with similar climatic conditions) without a deep regional and global synthesis. Thus, there is a lack of studies to generalize the effects of extreme weather events on GHG fluxes in different landscape types of polar latitudes under different climatic conditions using existing experimental data.

The main objective of our study is to assess the spatial variability in the response of the daily net ecosystem exchange (NEE) of CO<sub>2</sub>, GPP and RE between different tundra and forest tundra ecosystems of the Northern Hemisphere to extreme weather events, such as anomalous daily temperature and precipitation totals, during the growing season.

## 2. Materials and methods

To study the influence of daily temperature and precipitation extremes on CO<sub>2</sub> fluxes in tundra and forest-tundra ecosystems of the Northern Hemisphere, we used meteorological observations and eddy covariance flux measurements from 21 t stations of the global FLUXNET (<https://fluxnet.org/data/>, <https://fluxnet.org/data/fluxnet2015-dataset/>) and the regional AmeriFlux (<https://ameriflux.lbl.gov/>) networks.

Selected flux databases contain data on atmospheric CO<sub>2</sub> fluxes, key meteorological parameters, and information on local vegetation and soil characteristics (e.g., soil moisture). However, there are a significant number of gaps in the meteorological time series. At 11 monitoring stations there are no gaps in meteorological measurements, at 1 station there are no temperature measurements, and at 3 stations there are no precipitation measurements; at other stations the percentage of gaps ranges from 2% to 21% for temperature and from 6% to 30% for precipitation. To fill the gaps in the *in-situ* data, the ERA5 reanalysis data set was also used (Hersbach *et al* 2020). The ERA5 reanalysis was used in the study because it provides the longest data series (since 1950) and the best spatial resolution among all reanalyses (0.25 × 0.25 degrees). For example, the CRU dataset is gridded to

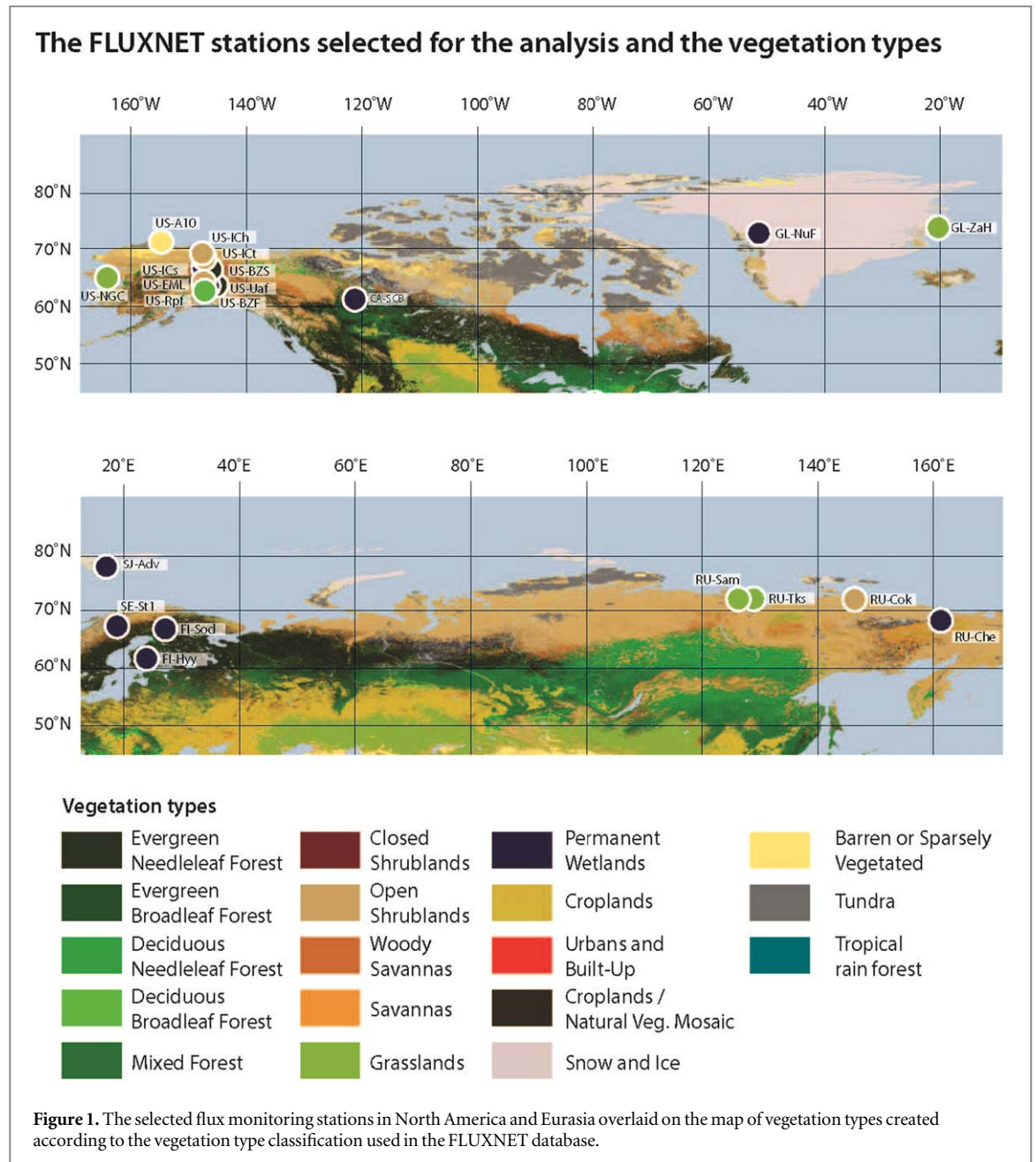
a resolution of  $0.5 \times 0.5$  degrees, while lower grid spacing is less suitable for the purposes of our study. Another reason for using the ERA5 reanalysis is that it was used in our two previous studies investigating the response of CO<sub>2</sub> fluxes to anomalous weather conditions in tropical and temperate ecosystems (Gushchina *et al* 2023a, 2023b). To allow comparison and generalization of all results, it was decided to use a common methodology and data sources for all latitudinal zones.

The strong agreement between the reanalysis and FLUXNET data sets for air temperature was demonstrated for most stations. The R-squared values for the temperature data sets exceed 0.95 for 15 stations and range from 0.88 to 0.94 for 5 stations at  $p < 0.05$  (Supplementary figure S1). The agreement between the precipitation rates obtained from the reanalysis and the monitoring stations is lower compared to the temperature. The R-squared values range between 0.04 and 0.70 at  $p < 0.05$  (Supplementary figure S2). Considering the low agreement between *in-situ* and reanalysis at some stations, we mainly used the precipitation and temperature data obtained at the corresponding experimental sites for our study. Existing gaps in the meteorological time series obtained from *in-situ* measurements were filled using the ERA5 reanalysis data set. To determine the air temperature and precipitation values at the FLUXNET sites, the mean values between 4 adjacent grid points of ERA5 data base were used. Daily mean air temperature was calculated from 3-hourly reanalysis data or 30-min observations at the monitoring stations. Daily precipitation totals were calculated as the daily sum of precipitation data from hourly reanalysis data or 30-min observations at the monitoring stations. Soil water content (SWC) data were obtained from field measurements at the FLUXNET sites. According to the FLUXNET monitoring standards, SWC is measured with standardized equipment at a depth of 10 cm. Measurements were taken at 30 min time intervals and averaged for each day.

To analyze the response of daily NEE in tundra and forest-tundra ecosystems to extreme weather events, 21 monitoring stations were selected. These stations have relatively long observation periods, are located in different landscapes and climatic conditions north of 60N (figures 1–2, table 1), and are also located in areas characterized by the most significant increase in the frequency of extreme weather events in recent decades (FAO 2020). The selected experimental sites belong to six biome types according to the international classification adopted by the International Geosphere-Biosphere Program (IGBP) and used in the FLUXNET network (Belward *et al* 1999): evergreen needleleaf forests, deciduous broadleaf forests, grasslands, permanent wetlands, open shrublands, and barren sparse vegetation. The maximum period of continuous flux observations at the selected stations was 18 years, the minimum - 2 years. More detailed characteristics of the vegetation and the length of the data time series at the flux monitoring stations are presented in table 1. It should be noted that this study focused only on the warm season of the year. The beginning and end of the warm season were defined as the sustained crossing of the daily mean air temperature of 0 °C for at least seven consecutive days.

The CO<sub>2</sub> flux data from the monitoring stations were analyzed according to international recommendations for processing eddy covariance data (Aubinet *et al* 2012). Average daily CO<sub>2</sub> flux values for each selected station were derived by averaging 30-minute measurements. Gaps in the flux data caused by equipment failure, weak turbulence, heavy precipitation, etc were filled using a machine learning model based on the gradient boosting-based model (CatBoost) to avoid systematic bias in the daily flux estimates at high latitudes according to Vekuri *et al* (2023). The model analyzes relationships between measured meteorological parameters obtained from site data and CO<sub>2</sub> flux values. By storing these patterns and combinations between existing flux values and meteorological parameters, gradient boosting effectively reconstructs missing NEE using the identified dependencies. We divided the data into test and training sets, where the training set contains meteorological data as training features and high-quality CO<sub>2</sub> flux data (without gaps) as target value. The model is trained and then tested on the prepared data sets. During the inference stage, the trained model performs gap-filling in the flux data using the corresponding meteorological information. Importantly, the meteorological characteristics used for inference are not included in the training dataset, thus avoiding data leakage. For a more detailed analysis of the influence of temperature and precipitation anomalies on CO<sub>2</sub> fluxes, the NEE of CO<sub>2</sub> was also partitioned into GPP and RE. The partitioning into these two components was performed using the Reddy Proc software package (Wutzler *et al* 2018).

Extreme temperature events were defined as intervals during which the daily mean temperature exceeded the 95% quantile (for extremely high temperatures) or failed to reach the 5% quantile (for extremely low temperatures) of the probability density function (Gushchina *et al* 2023a). Long-term temperature time series were analyzed assuming their normal distribution (Zheleznova and Gushchina 2023). Two approaches were used to determine the extreme precipitation threshold (Gushchina *et al* 2023b). The first approach defined extreme precipitation days as days with daily precipitation total exceeding the 95% quantile of the probability density function (the Weibull distribution was used for precipitation data). The second approach was based on the evaluation of the API (Antecedent Precipitation Index), which determines the cumulative effect of precipitation on CO<sub>2</sub> fluxes. The index was calculated following Li *et al* (2021):

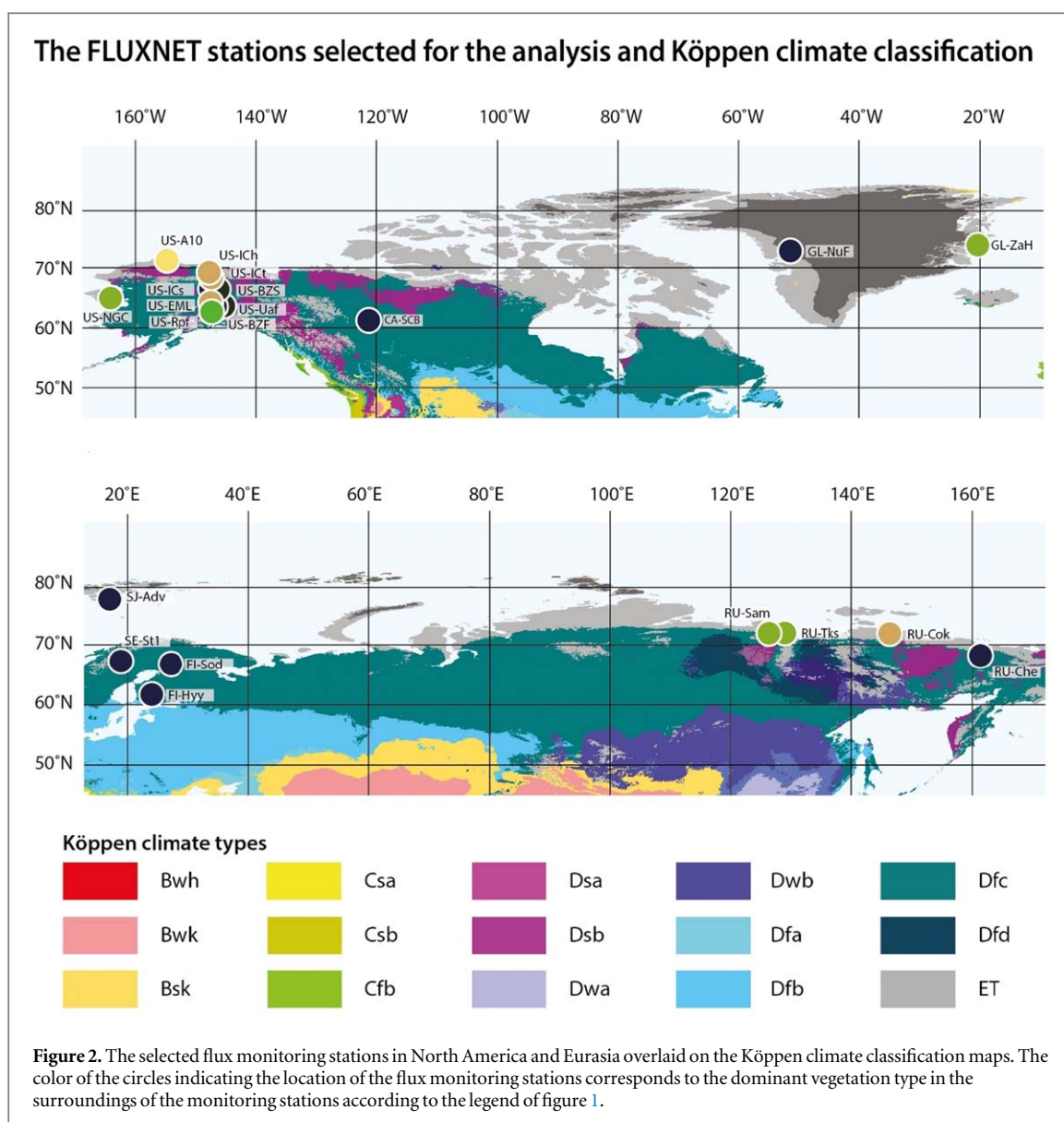


$$API = \sum_{t=1}^M P_t k^t,$$

where  $P_t$  is the sum of precipitation over the  $t$ th antecedent day;  $M$  is the number of antecedent days used for the calculation;  $k$  is the decay constant. In our study, we assumed that  $M$  is to be 14 days, and  $k$  is to be 0.8. (Gushchina *et al* 2023b). We identified extremely high (low) API days as those where the API value exceeded the 95% (below 5%) quantile of the empirical probability density function (PDF).

It is noteworthy that the analyzed time series contain two types of data: *in-situ* measurements and ERA5 reanalysis, which may have different PDF distributions and different 95/5% quantile thresholds (Supplementary figures S3, S4, S5). Therefore, for the temperature and precipitation time series, we computed the PDF distribution and defined the thresholds separately for reanalysis and *in-situ* data, using the *in-situ* threshold for the days with available observations at the stations and the reanalysis threshold for the days with gaps in temperature and precipitation measurements at the monitoring stations. We could not follow the same approach for API (different thresholds for days with *in-situ* and ERA data) because API is computed for 14-day intervals that may contain both *in-situ* and ERA5 data, so the thresholds for API were obtained from mixed time series and applied to all days. Different threshold definition methods were tested and the most appropriate method was selected (see details in the Supplementary, section Method of threshold definition).

Days with extremely high (low)  $\text{CO}_2$  fluxes were identified as days when the daily mean NEE value exceeded the 90% quantile (below 10%) of the empirical probability density function. The difference in the threshold for



meteorological and flux data (95/5% for temperature, precipitation and API and 90/10% for CO<sub>2</sub> fluxes) is due to the following reasons. Simultaneous extreme anomalies of temperature and precipitation can have opposite effects on fluxes, masking the CO<sub>2</sub> flux response. For example, it has been shown that high temperatures mostly lead to increased CO<sub>2</sub> emissions, while precipitation deficits in polar latitudes lead to increased CO<sub>2</sub> uptake. At the same time, high temperatures are usually associated with precipitation deficits, which have the opposite effect on CO<sub>2</sub> fluxes. This fact significantly reduces the number of days with simultaneous occurrence of extreme meteorological conditions and extreme fluxes, making the interpretation of the final statistic difficult. Therefore, the lower quantile threshold for fluxes was determined.

The empirical PDF distribution was used for API and NEE time series because their PDFs varied significantly among ecosystem types, making it difficult to select the most appropriate type of theoretical distribution. The PDF distribution for temperature, precipitation, and API was calculated separately for each calendar month and then averaged on a monthly basis over the period of available observations at each monitoring station. Therefore, the analyzed time period has the same length for meteorological and flux data time series at all monitoring stations considered.

### 3. Results and discussion

Analysis of CO<sub>2</sub> flux anomalies associated with periods of anomalous temperature and precipitation in tundra and forest-tundra ecosystems revealed a wide diversity of observed responses depending on geographic location, landscape type, and plant species composition.

**Table 1.** The FLUXNET stations selected for data analysis.

Station	Lat, long	Elev.m	Vegetation IGBP:	Climate type	Species composition	Period	References
FI-Hyy	61.84°N, 24.29°E	181	ENF, Evergreen Needleleaf Forests	Dfc, Subarctic	<i>Pinus sylvestris</i>	1996–2014	Suni <i>et al</i> (2003)
FI-Sod	67.36°N, 26.63°E	180		Dfc, Subarctic	<i>Pinus sylvestris</i>	2001–2014	Thum <i>et al</i> (2007)
US-BZS	64.69°N, –148.32°W	100		Dfd, Extremely cold subarctic	<i>Picea mariana</i>	2010–2021	Euskirchen (2022)
US-Uaf	64.86°N, –147.85°W	155		Dwc, Monsoon-influenced subarctic	<i>Picea mariana</i>	2003–2021	Chu <i>et al</i> (2021)
US-Rpf	65.11°N, –147.42°W	497	DBF, Deciduous Broadleaf forests	Dwc, Monsoon-influenced subarctic	<i>Rhododendron groenlandicum</i> , <i>Vaccinium uliginosum</i> , <i>Epilobium angustifolium</i> , <i>Carex</i> spp, <i>Betula papyrifera</i> var. <i>neoalaskana</i> , <i>Populus tremuloides</i> , <i>Salix</i> , <i>Picea mariana</i>	2008–2021	Chu <i>et al</i> (2021)
GL-ZaH	74.47°N, –20.55°W	38	GRA, Grasslands	ET, Polar tundra	<i>Cassiope tetragona</i> , <i>Dryas integrifolia</i> , <i>Vaccinium uliginosum</i> , <i>Salix arctica</i> , <i>Eriophorum scheuchzeri</i>	2000–2014	Lund <i>et al</i> (2012)
RU-Tks	71.59°N, 128.88°E	7		ET, Polar tundra	Not available	2010–2014	Aurela <i>et al</i> (2016)
RU-Sam	72.37°N, 126.49°E	0		ET, Polar tundra	<i>Hylocomium splendens</i> , <i>Dryas punctata</i> , <i>Peltigera</i> , <i>Polygonum viviparum</i> , <i>Saxifraga punctata</i> , <i>Astragalus frigidus</i>	2002–2014	Boike <i>et al</i> (2013)
US-NGC	64.86°N, –163.70°W	35		ET, Polar tundra	Not available	2017–2023	Torn and Dengel (2023)
RU-Cok	70.82°N, 147.49°E	48	OSH, Open Shrublands	Dfc, Subarctic	<i>Betula nana</i> , <i>Salix</i> sp., <i>Sphagnum</i> , <i>Potentilla palustris</i> , <i>Carex</i> , <i>Carex-Eriophorum</i>	2003–2014	van der Molen <i>et al</i> (2007)
US-ICt	68.60°N, –149.30°W	930		ET, Polar tundra	<i>Eriophorum vaginatum</i> , <i>Sphagnum</i> spp., <i>Betula nana</i> , <i>Salix</i> spp., <i>Rhododendron subarcticum</i> , <i>Vaccinium vitis-idaea</i>	2007–2021	Euskirchen <i>et al</i> (2017)
US-EML	63.87°N, –149.25°W	700		ET, Polar tundra	<i>Eriophorum vaginatum</i> , <i>Vaccinium uliginosum</i> , <i>Rubus chamaemorus</i> , <i>Betula nana</i> , <i>Ledum palustre</i> , <i>Sphagnum</i> spp., <i>Dicranum</i> spp	2008–2020	Belshe <i>et al</i> (2012)
US-ICb	68.60°N, –149.29°W	940		ET, Polar tundra	<i>Eriophorum vaginatum</i> , <i>Sphagnum</i> spp., <i>Betula nana</i> , <i>Salix</i> spp., <i>Rhododendron subarcticum</i> , <i>Vaccinium vitis-idaea</i>	2007–2021	Euskirchen <i>et al</i> (2017)
RU-Che	68.61°N, 161.34°E	6	WET, Permanent Wetlands	Dfc, Subarctic	<i>Carex appendiculata</i> , <i>Potentilla palustris</i> , <i>Eriophorum angustifolium</i> , <i>Betula nana</i> , <i>Salix</i> , <i>Sphagnum</i>	2002–2005	Merbold <i>et al</i> (2009)
US-BZF	64.70°N, –148.31°W	95		Dfd, Extremely cold subarctic	<i>Equisetum</i> , <i>Carex</i> , <i>Potentilla</i> , <i>Sphagnum</i>	2011–2021	Euskirchen <i>et al</i> 2020
US-ICs	68.60°N, –149.31°W	920		ET, Polar tundra	<i>Eriophorum vaginatum</i> , <i>Sphagnum</i> spp., <i>Betula nana</i> , <i>Salix</i> spp., <i>Rhododendron subarcticum</i> , <i>Vaccinium vitis-idaea</i>	2007–2021	Euskirchen <i>et al</i> (2017)
SE-St1	68.35°N, 19.05°E	351		Dfc, Subarctic	<i>Empetrum hermaphroditum</i> , <i>Betula nana</i> , <i>E. vaginatum</i> , <i>Carex rotundata</i> , <i>E. vaginatum</i> , <i>E. angustifolium</i>	2012–2014	Johansson <i>et al</i> (2006)
SJ-Adv	78.18°N, 15.92°E	17		ET, Polar tundra	Not available	2011–2014	Christensen (2016)

Table 1. (Continued.)

Station	Lat, long	Elev.m	Vegetation IGBP:	Climate type	Species composition	Period	References
GL-NuF	64.13°N, −51.38°W	50		ET, Polar tundra	<i>Scirpus cespitosus</i> , <i>Empetrum nigrum</i> , <i>Vaccinium uliginosum</i> , <i>Salix glauca</i> , <i>S. glauca</i>	2008–2014	López-Blanco <i>et al</i> (2017)
CA-SCB	61.30°N, −121.29°W	280		Dfc, Subarctic	<i>Not available</i>	2014–2019	Torn and Dengel (2022)
US-A10	71.32°N, −156.61°W	4	BSV, Barren Sparse Vegetation	ET, Polar tundra	<i>Carex aquatilis</i> , <i>Sphagnum sp.</i>	2011–2020	Bao <i>et al</i> (2021)

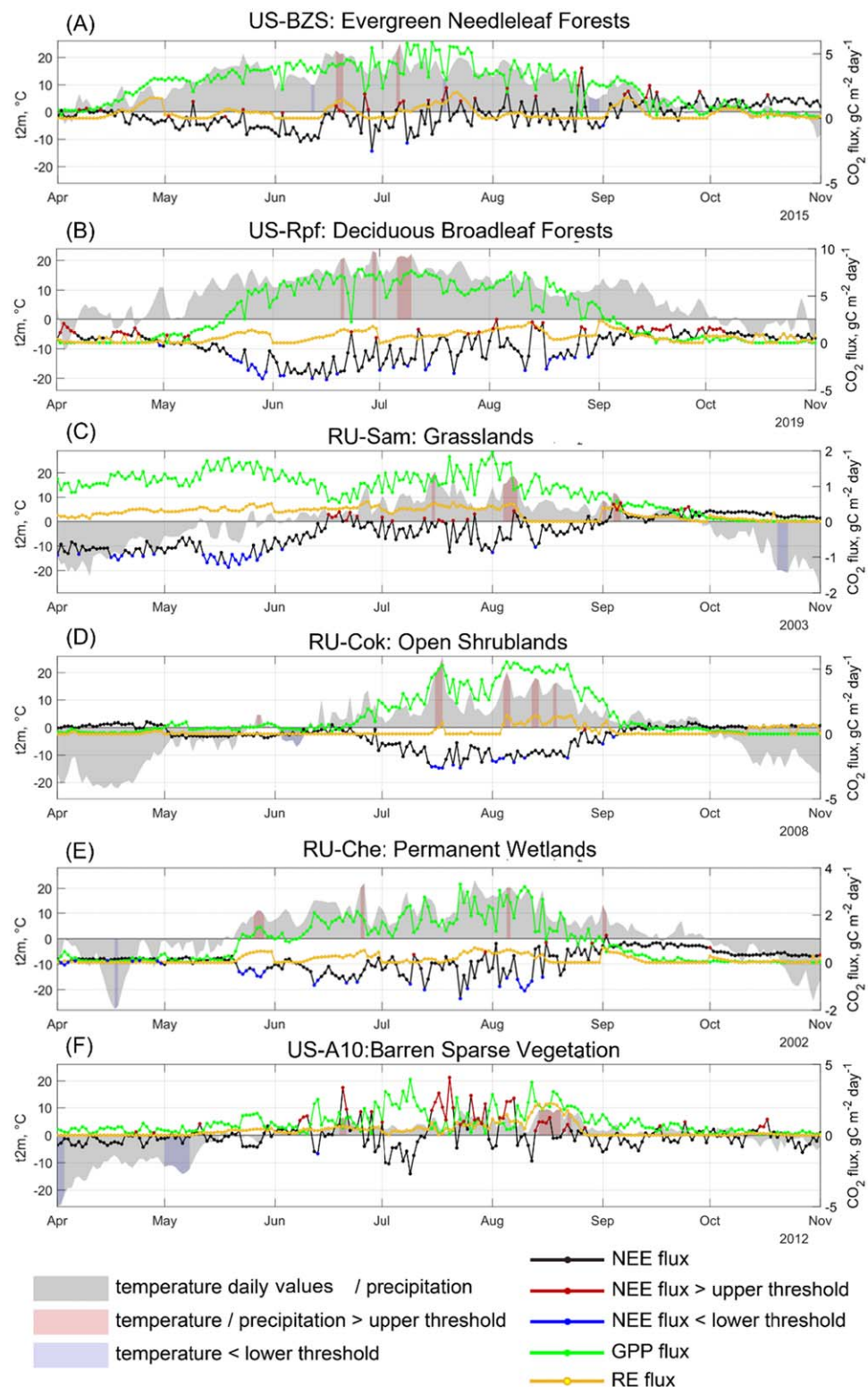
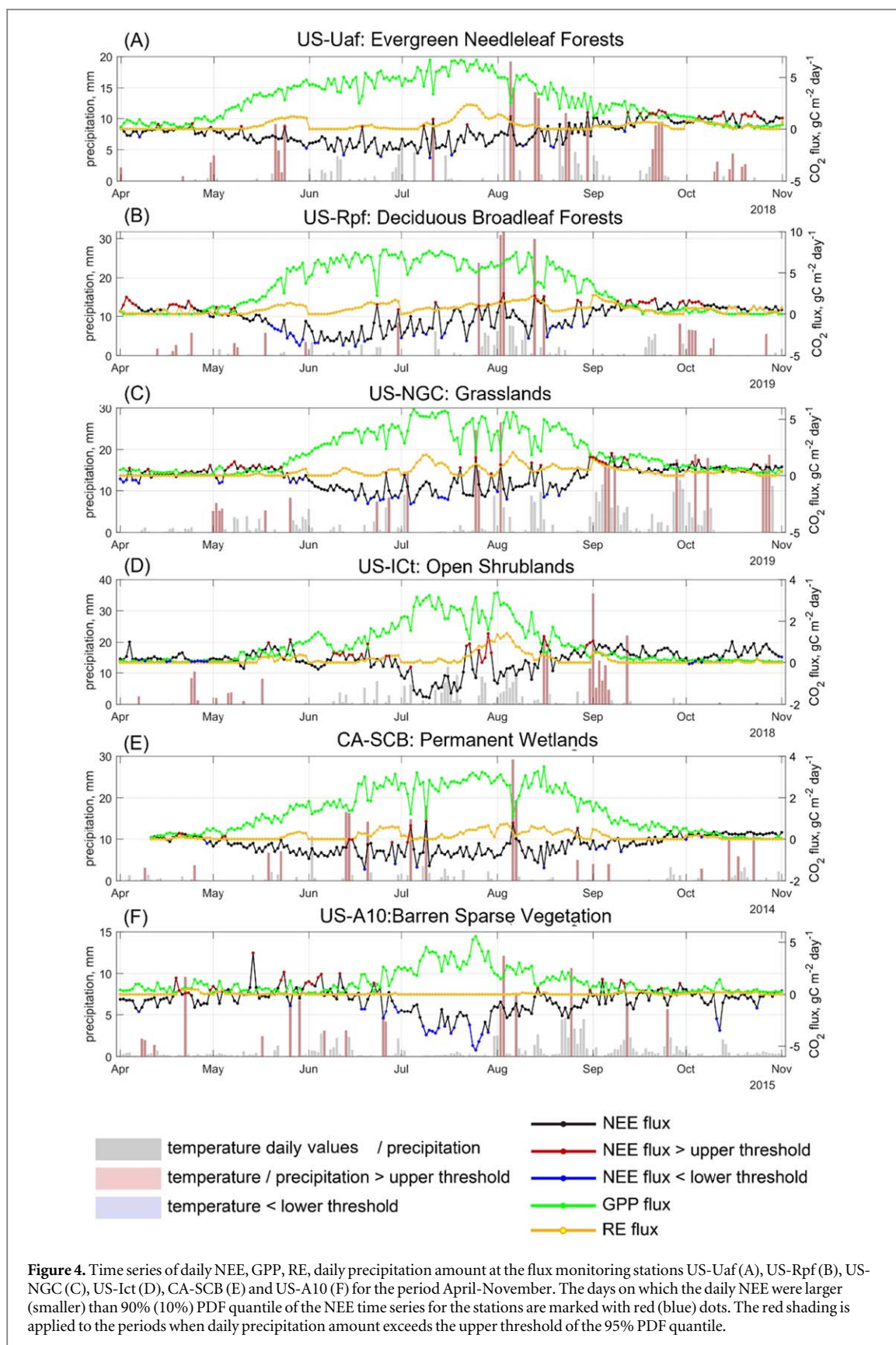
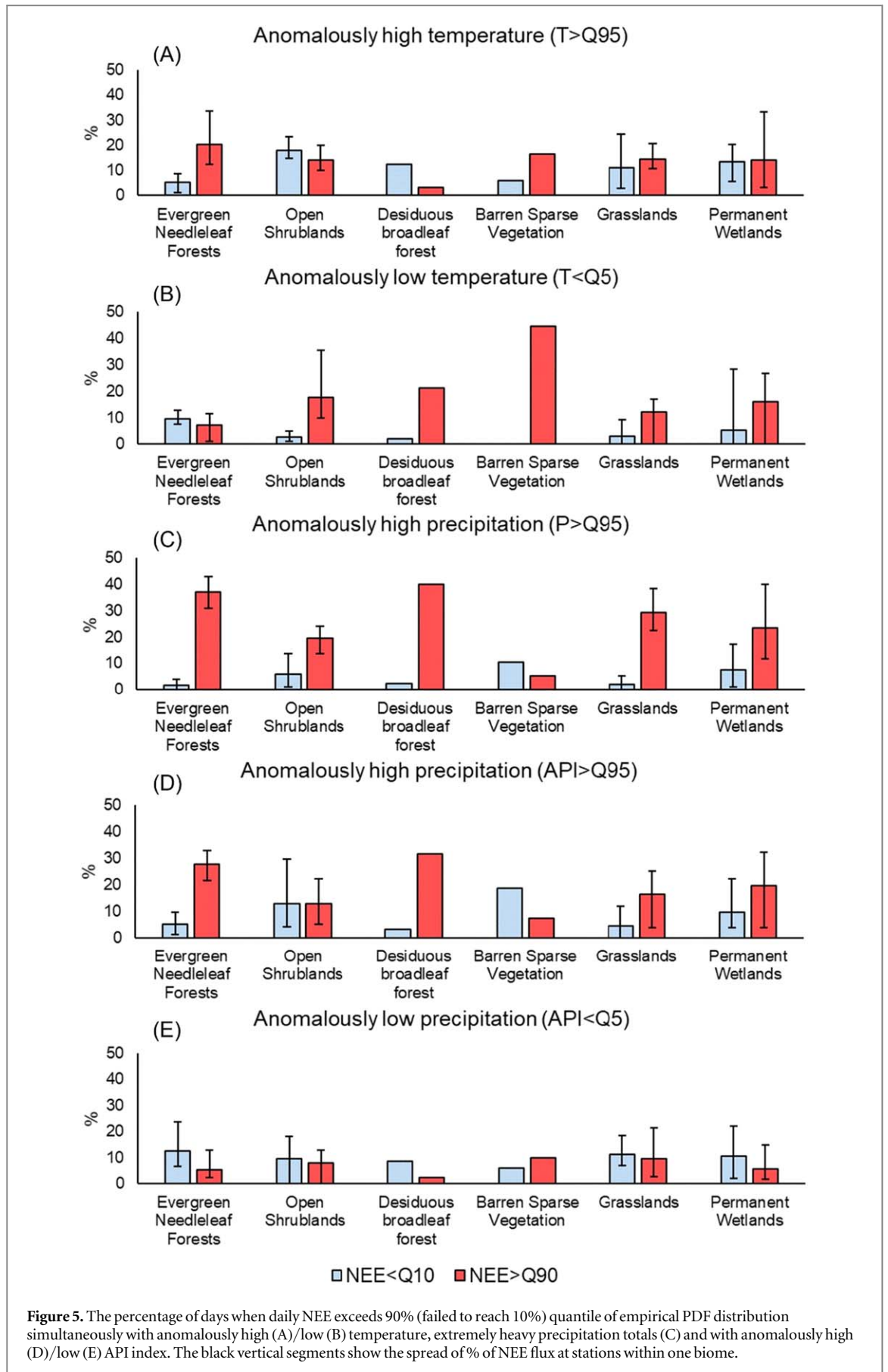


**Figure 3.** Time series of daily NEE, GPP, RE, daily temperature totals at the flux monitoring stations US-BZF (A), US-Rpf (B), Ru-Sam (C), Ru-Cok (D), Ru-Che (E) and US-A10 (F) for the period April–November. The days on which the daily NEE were larger (smaller) than 90% (10%) PDF quantile in the NEE time series for the stations are marked with red (blue) dots. The red (blue) shading is applied to the periods when temperature exceeds the upper (lower) threshold of the 95% (5%) PDF quantile.

During the warm season, increases in GPP and RE were observed in most of the ecosystems considered as a result of increased solar radiation and associated rises in air temperature and soil moisture (figures 3–4). It was also shown that the response of GPP and RE to the temperature and precipitation anomalies differed significantly, resulting in different impacts on NEE.



The response of CO<sub>2</sub> fluxes to anomalously high temperatures varies across biomes. In deciduous broadleaf forests and open shrublands, extremely low NEE (lower than 10% quantile) occur more frequently than high NEE, being observed on 12%–23% of the days with anomalously high temperatures (figure 5(A)). It should be noted that NEE lower than 10% quantile can be interpreted as both increased CO<sub>2</sub> uptake and decreased CO<sub>2</sub> release, depending on the sign of the daily NEE (similarly, positive NEE can be associated with increased CO<sub>2</sub>



emission and decreased uptake). To avoid this uncertainty, we show table S1 and table S2 in the Supplementary Materials, where the sign of the NEE quantile is considered for each day. For most stations in these two considered biomes, the lower 10% quantile of NEE corresponds to enhanced CO<sub>2</sub> uptake during the summer months, when the anomalously high temperatures occur more frequently (table S2). This effect can be attributed to the thermal regime of the polar region, where anomalously high temperatures (exceeding the 95% quantile) are found in the range of 23 °C–25 °C, which do not lead to thermal stress for the vegetation, but on the contrary contribute to a higher plant photosynthesis rate, resulting in a stronger increase of GPP compared to RE (under sufficient soil moisture in the plant root zone) and thus a strongly negative NEE (figure 3BD).

In evergreen needleleaf forests, grasslands and ecosystems with barren, sparse vegetation, hot periods are associated with anomalously high NEE exceeding the 90% quantile (figure 5(A)). According to table S1, at most stations located in these vegetation zones this corresponds to enhanced CO<sub>2</sub> emission, while only at the stations Fi-Hyy, US-Uaf and US-NGC in 27%–46% of cases the NEE > 90% quantile is observed at the days with negative NEE, that corresponds to weakened CO<sub>2</sub> uptake. Such a response to anomalously high temperatures in evergreen needleleaf forests may be due to the more southerly location of these biomes compared to other stations, resulting in a higher temperature threshold (>25 °C). These temperatures can induce thermal plant stress and a consequent weakening of plant photosynthesis and dark respiration, as well as either reduced or increased soil respiration, which may result in increased release of CO<sub>2</sub> from the ecosystem to the atmosphere (Teskey *et al* 2015, Anjileli *et al* 2021) (figure 3(A)). A similar response was found by Heiskanen *et al* (2023) in a pine forest in northern Finland during a heat wave. In the barren, sparse vegetation sites, the anomalously high NEE under high temperature may be due to enhanced CO<sub>2</sub> emission from melting permafrost (figure 3(F)). In grasslands, increased emissions associated with high temperatures may also result from suppressed photosynthesis of tundra vegetation due to anomalously hot conditions (figure 3(C)). Other reasons for the opposite NEE response to temperature increase in evergreen needleleaf forests, grasslands, and ecosystems with barren, sparse vegetation compared to deciduous broadleaf forests and open shrublands may be the different adaptive capacity of vegetation types and soil moisture conditions.

In the permanent wetlands, the same percentage of days with anomalously low and high NEE is observed under anomalously high temperatures (figure 5(A)). The NEE < 10% quantile occurs when the temperature increase results in a strong increase in GPP, while the NEE > 90% quantile is associated with the period of high RE and relatively low GPP under high temperature, which is more characteristic of the beginning or the end of the warm period (figure 3(E)). A similar response of increased CO<sub>2</sub> emissions due to anomalous temperature values in polar ecosystems was also found in the works of Schuur *et al* (2015) and Elberling *et al* (2008).

The effect of the anomalously low temperature on the CO<sub>2</sub> fluxes consists of anomalously high NEE outnumbering low ones (figure 5(B)). This is mostly associated with increased CO<sub>2</sub> emission (table S1). A similar effect at low temperatures was also observed in the work of Natali *et al* (2019). This response may be related to the suppressed photosynthesis at low temperatures, especially during summer frosts, which are quite frequent in polar regions. This fact is confirmed by the strong decrease in GPP observed during cold periods, while RE does not show significant changes (figure S7B, D). In evergreen needleleaf forests, CO<sub>2</sub> uptake dominates CO<sub>2</sub> release during the period of anomalously low temperatures (figure 5(B)). As mentioned above, the evergreen needleleaf forest stations are located at the southern boundary of the polar zone, where the anomalously low summer temperatures do not fall below 0 °C and thus do not lead to cold stress for photosynthetic processes.

Two approaches were used to analyze the response of tundra and tundra-forest ecosystems to precipitation anomalies. First, the simultaneous effect of heavy precipitation was considered by selecting days with daily precipitation totals exceeding the 95% quantile of the PDF. The cumulative effect of precipitation on CO<sub>2</sub> fluxes was defined using the API index. The simultaneous response of CO<sub>2</sub> fluxes to heavy precipitation (>95% quantile) is manifested in an increased CO<sub>2</sub> emission into the atmosphere at almost all stations considered: up to 42% of the days with heavy precipitation coincide with daily NEE > 90% quantile (figure 5(C)). This fact is confirmed by the analysis of the time series of precipitation and NEE (figures 4(A)–(E)), where the increased precipitation coincides with anomalously high NEE (CO<sub>2</sub> emission into the atmosphere). The observed response can be explained by the ‘Birch effect’ (Birch 1964), which consists in the intensification of soil respiration due to the strong increase in soil moisture and the consequent enhanced rates of decomposition and mineralization associated with heavy rainfall and rising groundwater levels (Manzoni *et al* 2020). The exception is the barren sparse vegetation ecosystems, where the NEE < 10% quantile dominates the NEE > 95% quantile (figures 4(F), 5(C)) during days with heavy precipitation and soil wetting. The increased CO<sub>2</sub> uptake associated with heavy precipitation may be due to the rapid response of these plant communities to soil wetting, as well as the reduced response of soil heterotrophic respiration to precipitation.

The cumulative effect of heavy precipitation (API > 95% quantile) on NEE flux is similar to the simultaneous effect, i.e., heavy precipitation during the preceding 14 days mostly leads to anomalously high NEE (higher CO<sub>2</sub> emission), which dominate the CO<sub>2</sub> uptake in ecosystems of evergreen needleleaf forest, deciduous broadleaf forest, grasslands and permanent wetlands (figure 5(D)). It should be noted, however, that the

percentage of days when increased CO<sub>2</sub> uptake follows the period of heavy precipitation is significantly higher than for the simultaneous NEE response to precipitation on a daily scale. The increased CO<sub>2</sub> uptake following the period of heavy rainfall may be due to the increased rate of photosynthesis that occurs under sunny weather and optimal soil moisture conditions (Zscheischler *et al* 2014).

The prolonged precipitation deficit, characterized by low API values, is accompanied by strongly negative NEE in the majority of the considered tundra and forest-tundra ecosystems, corresponding to increased CO<sub>2</sub> uptake (figure 5(E)). On the one hand, this demonstrates the high adaptive capacity of the considered polar ecosystems to the short-term (less than 14 days) precipitation deficit. On the other hand, the low cloudiness associated with periods of precipitation deficit may contribute to increased solar radiation and thus to intensified photosynthesis in these ecosystems and consequently to increased CO<sub>2</sub> uptake.

The precipitation deficit results in anomalously high positive rather than anomalously low negative NEE at some stations located in the permafrost zone (RU-Che, Ru-Tks and US-A10) (Figure S8). At these sites, the increased ecosystem respiration (RE) may be influenced by the intensification of heterotrophic respiration due to the contribution of melting permafrost soils rich in organic matter (Schädel *et al* 2016, Natali *et al* 2019).

For a deeper analysis of the effect of high and low temperature, as well as the effect of excess and deficient precipitation on CO<sub>2</sub> fluxes in different polar ecosystems, we plotted the scatter plots for a few selected stations (the most representative stations for each biome) showing the dependence of NEE on air temperature and soil water content (SWC) (figure 6). SWC is one of the most important parameters in the hydrological cycle, depending on the amount of precipitation received and directly affecting plant functions and growth. It has a direct effect on the GPP and RE of plant ecosystems, allowing a more comprehensive analysis of the relationships between NEE and different environmental variables.

The largest effect of temperature on NEE at high soil moisture values was found for grassland ecosystems (e.g., station US-NGC taken as an example): at temperatures above 10 °C, grasslands serve as a CO<sub>2</sub> sink, while at temperatures below 5 °C - as a CO<sub>2</sub> source (figure 6(a)). This NEE response is a result of the close relationship between plant photosynthesis and temperature. At the experimental site, maximum plant photosynthesis and GPP increase are recorded when the temperature reaches the 10 °C threshold in case of sufficient soil moisture conditions. At the same time, the emission of CO<sub>2</sub> is increased under reduced soil moisture availability, and NEE in this case is mainly controlled by changes in RE. Similar relationships between temperature, soil moisture and NEE were found at the RU-Tks station. However, the relationships found at the GL-ZaH flux monitoring station are different from those discussed above: NEE is affected by temperature variation, but at low soil moisture. The different response may be due to the more northerly location of this experimental site (74°N), the limited range of temperature variation (from -5 to 10 °C) and the prevailing soil overwetting conditions during the growing season.

The dependence of CO<sub>2</sub> fluxes on temperature and soil moisture in wetlands is similar to that in grasslands. At the US-BZF station, the clear relationship between temperature and NEE is observed at high soil moisture: when soil moisture is above 90% and temperature is above 15 °C, ecosystem uptake of CO<sub>2</sub> is sustained (figure 6(b)). Conversely, CO<sub>2</sub> emission dominates at temperatures below 10 °C, as well as during the prolonged dry periods when soil moisture decreases to 5%–10%. The analogous response was observed at the US-ICs experimental site. Similar results were found in the study of Lafleur *et al* (2003), where an increase in RE was also observed under drought conditions. In the Canadian wetlands (CA-SCB), soil moisture does not affect CO<sub>2</sub> fluxes at all, which may be related to the over-watering of the peatland during the warm season. At this station sustainable CO<sub>2</sub> uptake occurs when the temperature exceeds 10 °C. The study by Lund *et al* (2010) also notes that in polar permanent wetland ecosystems, the high groundwater table suppresses the rate of microbial decomposition, making the wetland a CO<sub>2</sub> sink.

The open shrubland ecosystems of Alaska (US-ICt, US-ICb and US-NGC) are characterized by the same relationship between temperature, soil moisture and NEE as wetlands and grasslands. The response is different for the US-EML experimental site, where temperature variations during the growing season govern the CO<sub>2</sub> exchanges that manifest at both low and high soil moisture conditions. At temperatures above 10 °C (regardless of moisture content), CO<sub>2</sub> uptake occurs in this ecosystem, while at temperatures below 10 °C, CO<sub>2</sub> emission into the atmosphere prevails. This finding is most likely due to the high adaptive capacity of vegetation in this ecosystem to long dry periods, as well as over-wetting of the soil. A similar sustainable ecosystem response to the variation of temperature and moisture conditions is observed in North Alaska at the US-A10 station, which belongs to the barren sparse vegetation type. Only negative temperatures during the warm season (in the absence of snow cover) are associated with CO<sub>2</sub> emission, while after the temperature transition to zero, plant CO<sub>2</sub> uptake again prevails.

The analysis of forest-tundra ecosystems in polar latitudes (evergreen needleleaf forest) showed no clear dependence of NEE on temperature and soil moisture (figure S9). The response varies with geographic location, climatic conditions, and vegetation type. At the US-Uaf station, air temperature has a significant effect on the sign of NEE (figure 6(e)): when it is higher than 7 °C (regardless of soil moisture), ecosystems CO<sub>2</sub> uptake

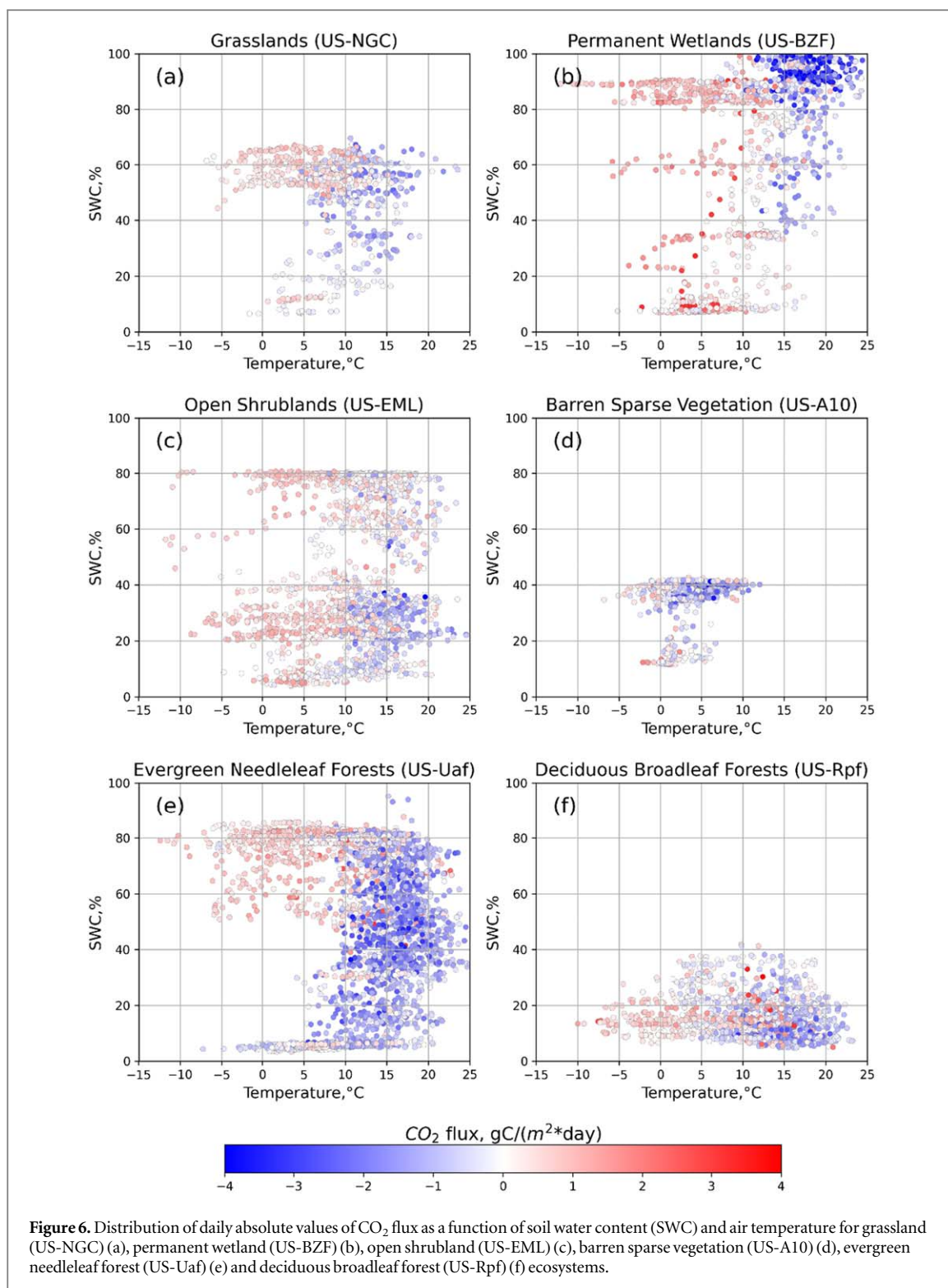


**Figure 6.** Distribution of daily absolute values of CO<sub>2</sub> flux as a function of soil water content (SWC) and air temperature for grassland (US-NGC) (a), permanent wetland (US-BZF) (b), open shrubland (US-EML) (c), barren sparse vegetation (US-A10) (d), evergreen needleleaf forest (US-Uaf) (e) and deciduous broadleaf forest (US-Rpf) (f) ecosystems.

prevails. Overwetting of the soil together with low temperatures leads to prevailed CO<sub>2</sub> emission. The similar response is observed at US-BZS, also located in Alaska. However, increased temperature is not always associated with increased CO<sub>2</sub> uptake, but can also result in positive NEE. At the FI-Hyy and FI-Sod stations in Finland, no dependence on soil moisture was found. The more southerly FI-Hyy site serves as a CO<sub>2</sub> sink when the temperature rises above 10 °C, while at FI-Sod, located in northern Finland, the anomalously high temperatures lead to CO<sub>2</sub> release. In deciduous broadleaf forests (US-Rpf experimental site), the relationship between CO<sub>2</sub> flux, temperature and moisture conditions was consistent with that observed at the FI-Sod station (figure 6(d)).

To summarize, the temperature effect on CO<sub>2</sub> fluxes dominates the effect of soil moisture in tundra and forest-tundra ecosystems of polar latitudes. It is noteworthy that the temperature increase above the threshold (about +10 °C on average for all considered sites) contributes to the intensification of photosynthesis rate and

enhanced CO<sub>2</sub> uptake, while the anomalously low temperature observed during the warm period, on the contrary, leads to the increased CO<sub>2</sub> emission. The effect of increasing CO<sub>2</sub> uptake by tundra ecosystems with increasing temperature was also found in the work of Oechel *et al* (2000). The effect of soil moisture is manifested in increased CO<sub>2</sub> emissions due to soil drying across all tundra and forest-tundra ecosystems.

#### 4. Conclusion

Analysis of CO<sub>2</sub> fluxes in tundra and forest-tundra ecosystems revealed a wide range of observed responses of NEE to anomalous temperature and precipitation events during the growing season, depending on geographic location and landscape type.

While most previous studies (Elberling *et al* 2008, Schuur *et al* 2015) documented the effect of suppressed photosynthesis associated with anomalously high temperatures and consequently increased CO<sub>2</sub> emissions in polar ecosystems, we observed the similar reduced CO<sub>2</sub> uptake only in forest-tundra ecosystems at the southern boundary of the polar region, where heat waves are more frequent, and in ecosystems with barren sparse vegetation and grasslands. The opposite response was found in deciduous broadleaf forests and open shrublands, where CO<sub>2</sub> uptake prevailed on 13%–23% of the anomalously high temperature days. This effect can be attributed to the temperature regime of the polar region with not very high air temperatures, which do not lead to heat stress for the vegetation, but on the contrary contribute to a higher increase of GPP compared to RE. This effect was also found in the study by Oechel *et al* (2000), but not for extreme temperature periods.

The effect of the anomalously low temperature on the CO<sub>2</sub> fluxes is that the anomalously high NEE occur more frequently than the low ones, which is mostly associated with an increase in CO<sub>2</sub> emissions due to the lower GPP.

We differentiated the simultaneous and cumulative effects of heavy precipitation on CO<sub>2</sub> fluxes in polar ecosystems. It was shown that the response of CO<sub>2</sub> fluxes to anomalously high and low precipitation is rather similar regardless of the time scale (short-term or long-term response). The simultaneous response of CO<sub>2</sub> fluxes to heavy precipitation is manifested in increased CO<sub>2</sub> emissions to the atmosphere for most of the ecosystems studied: up to 42% of the days with heavy precipitation coincide with the NEE > 90% quantile. The cumulative effect of heavy precipitation on the NEE flux is similar to the simultaneous effect, i.e., heavy precipitation during the preceding 14 days mostly leads to positive daily NEE > 90% quantile (higher CO<sub>2</sub> emission), which dominates the negative NEE < 10% quantile in the ecosystems of evergreen needleleaf forest, deciduous broadleaf forest, grasslands and permanent wetlands. It should be noted, however, that the percentage of days with increased CO<sub>2</sub> uptake following the period of heavy precipitation is significantly higher than for the simultaneous NEE response to precipitation on a daily scale. The prolonged precipitation deficit, characterized by low API values is associated with negative NEE < 10% quantiles in the majority of tundra and forest-tundra ecosystems considered, corresponding to increased CO<sub>2</sub> uptake.

The present study covers only a small part of the existing natural diversity of CO<sub>2</sub> flux-exchange processes in polar ecosystems, which are characterized by great diversity and differences in the response of plant ecosystems to environmental changes. It is clear that further sophisticated studies with larger flux data sets and longer monitoring time series are urgently needed.

#### Acknowledgments

This research was funded by the Russian Science Foundation, grant number 22–17–00073.

#### Data availability statement

All data that support the findings of this study are included within the article (and any supplementary files).

#### ORCID iDs

Elizaveta Gorbarenko  <https://orcid.org/0009-0009-7086-2814>

Daria Gushchina  <https://orcid.org/0000-0002-9892-2040>

Maria Tarasova  <https://orcid.org/0000-0003-1507-3088>

Irina Zheleznova  <https://orcid.org/0000-0002-4495-8742>

Ravil Gibadullin  <https://orcid.org/0009-0005-0496-1970>

Alexander Osipov  <https://orcid.org/0000-0002-6659-2921>

Alexander Olchev  <https://orcid.org/0000-0002-6144-5826>

## References

- Anjileli H, Huning L S, Moftakhari H, Ashraf S, Asanjan A A, Norouzi H and AghaKouchak A 2021 Extreme heat events heighten soil respiration *Sci Rep.* **11** 6632
- Arndt K A, Lipson D A, Hashemi J, Oechel W C and Zona D 2020 Snow melt stimulates ecosystem respiration in Arctic ecosystems *Glob Change Biol* **26** 5042–51
- Aubinet M, Vesala T and Papale D 2012 *Eddy Covariance: A Practical Guide to Measurement and Data Analysis* (Springer) 438
- Aurela M, Laurila T, Hatakka J, Tuovinen J P and Rainne J 2016 FLUXNET2015 RU-Tks Tiksi FluxNet Dataset (<https://doi.org/10.18140/FLX/1440244>)
- Bao T, Xu X, Jia G, Billesbach D P and Sullivan R C 2021 Much stronger tundra methane emissions during autumn freeze than spring thaw *Glob. Change Biol* **27** 376–87
- Belshe E F, Schuur E A G, Bolker B M and Bracho R 2012 Incorporating spatial heterogeneity created by permafrost thaw into a landscape carbon estimate *J. Geophys. Res.: Biogeosciences* **117** G1
- Belward A S, Estes J and Kline K 1999 The 1GB P-DIS global 1-km land-cover data set DISCover: a project overview *Photogramm. Eng. Remote Sens.* **65** 1013–20
- Berner L T, Beck P S A, Loranty M M, Alexander H D, Mack M C and Goetz S J 2012 Cajander larch (*Larix cajanderi*) biomass distribution, fire regime and post-fire recovery in northeastern Siberia *Biogeosciences* **9** 3943–59
- Birch H F 1964 Mineralisation of plant nitrogen following alternate wet and dry conditions *Plant Soil* **20** 43–9
- Bjerke J W et al 2014 Record-low primary productivity and high plant damage in the nordic Arctic region in 2012 caused by multiple weather events and pest outbreaks *Environ. Res. Lett.* **9** 084006
- Boike J et al 2013 Baseline characteristics of climate, permafrost and land cover from a new permafrost observatory in the Lena River Delta, Siberia (1998–2011) *Biogeosciences* **10** 2105–28
- Bokhorst S, Bjerke J W, Street L E, Callaghan T V and Phoenix G K 2011 Impacts of multiple extreme winter warming events on sub-Arctic heathland: phenology, reproduction, growth, and CO<sub>2</sub> flux responses *Glob. Change Biol.* **17** 2817–30
- Bokhorst S, Cornelissen J H C and Veraverbeke S 2022 Long-term legacies of seasonal extremes in Arctic ecosystem functioning *Glob. Change Biol.* **28** 3161–2
- Bolan S et al 2024 Impacts of climate change on the fate of contaminants through extreme weather events *Sci. Total Environ.* **909** 168388
- Braybrook C A, Scott N A, Treitz P M and Humphreys E R 2021 Interannual variability of summer net ecosystem CO<sub>2</sub> exchange in High Arctic tundra *Journal of Geophysical Research: Biogeosciences* **126** e2020JG006094
- Chapin F S III et al 2005 Role of land-surface changes in Arctic summer warming *Science* **310** 657–60
- Christensen T 2016 FLUXNET2015 SJ-Adv adventdalen FluxNet NATEKO Lund University Dataset (<https://doi.org/10.18140/flx/1440241>)
- Chu H et al 2021 Representativeness of eddy-covariance flux footprints for areas surrounding ameriflux sites *Agric. For. Meteorol.* **301–302** 108350
- Davis E L and Gedalof Z E 2018 Limited prospects for future alpine treeline advance in the canadian rocky mountains *Glob. Change Biol.* **24** 4489–504
- Dobricic S, Russo S, Pozzoli L, Wilson J and Vignati E 2020 Increasing occurrence of heat waves in the terrestrial Arctic *Environ. Res. Lett.* **15** 024022
- Dvornikov Y, Novenko E, Korets M and Olchev A 2022 Wildfire dynamics along a north-central siberian latitudinal transect assessed using landsat imagery *Remote Sensing* **14** 790
- Elberling B et al 2008 High-Arctic soil CO<sub>2</sub> and CH<sub>4</sub> production controlled by temperature, water, freezing and snow *Advances in Ecological Research* **40** 441–72
- Euskirchen E S 2022 AmeriFlux BASE US-BZS bonanza creek black spruce Ver. 3-5 AmeriFlux AMP dataset [10.17190/AMF/1756434](https://doi.org/10.17190/AMF/1756434)
- Euskirchen E S, Bret-Harte M S, Shaver G R, Edgar C W and Romanovsky V E 2017 Long-term release of carbon dioxide from Arctic tundra ecosystems in alaska *Ecosystems* **20** 960–74 doi:
- Euskirchen E S, Kane E S, Edgar C W and Turetsky M R 2020 When the source of flooding matters: divergent responses in carbon fluxes in an Alaskan rich fen to two types of inundation *Ecosystems* **23** 1138–53
- FAO 2020 *Global Forest Resources Assessment 2020: Main report* (FAO) 11–23
- Francis J A, Vavrus S J and Cohen J 2017 Amplified Arctic warming and mid-latitude weather: new perspectives on emerging connections *Wiley Interdiscip. Rev. Clim. Change* **8** e474
- Friedlingstein P et al 2023 Global carbon budget 2023 *Earth Syst. Sci. Data* **15** 5301–69
- Gushchina D, Tarasova M, Satosina E, Zheleznova I, Emelianova E, Gibadullin R, Osipov A and Olchev A 2023b The response of daily carbon dioxide and water vapor fluxes to temperature and precipitation extremes in temperate and boreal forests *Climate* **11** 206
- Gushchina D, Tarasova M, Satosina E, Zheleznova I, Emelianova E, Novikova E and Olchev A 2023a Effects of extreme temperature and precipitation events on daily CO<sub>2</sub> fluxes in the tropics *Climate* **11** 117
- Heiskanen L et al 2023 Meteorological responses of carbon dioxide and methane fluxes in the terrestrial and aquatic ecosystems of a subArctic landscape *Biogeosciences* **20** 545–72
- Hersbach H B et al 2020 The ERA5 global reanalysis *Q. J. R. Meteorolog. Soc.* **146** 1999–2049
- Hollister R D, Webber P J and Tweedie C E 2005 The response of Alaskan Arctic tundra to experimental warming: differences between short- and long-term responses *Glob. Change Biol.* **11** 525–36
- IPCC 2022 *Climate Change 2022: Impacts, Adaptation, and Vulnerability. Contribution of Working Group II to the Sixth Assessment Report of the Intergovernmental Panel on Climate Change* [H.-O. Pörtner, D.C. Roberts, M. Tignor, E.S. Poloczanska, K. Mintenbeck, A. Alegría, M. Craig, S. Langsdorf, S. Löschke, V. Möller, ed A Okem and B Rama (Cambridge University Press) 3056
- Jarvis et al 2007 Drying and wetting of mediterranean soils stimulates decomposition and carbon dioxide emission: the 'Birch effect' *Tree Physiol.* **27** 929–40
- Johannessen et al 2004 Arctic climate change: observed and modelled temperature and sea-ice variability *Tellus A: Dynamic Meteorology and Oceanography* **56** 328–41
- Johansson T, Malmer N, Crill P M, Friborg T, Åkerman J H, Mastepanov M and Christensen T R 2006 Decadal vegetation changes in a northern peatland, greenhouse gas fluxes and net radiative forcing *Glob change biol* **12** 2352–69
- Kwon M J et al 2021 Siberian 2020 heatwave increased spring CO<sub>2</sub> uptake but not annual CO<sub>2</sub> uptake *Environ. Res. Lett.* **16** 124030
- Lafleur P M, Roulet N T, Bubier J L, Froking S and Moore T R 2003 Interannual variability in the peatland-atmosphere carbon dioxide exchange at an ombrotrophic bog *Global Biogeochem. Cycles* **17** 2
- Li W et al 2022 Widespread increasing vegetation sensitivity to soil moisture *Nat. Commun.* **13** 3959

- Li X, Wei Y and Li F 2021 Optimality of antecedent precipitation index and its application *J. Hydrol.* **595** 126027
- Liu Z et al 2020 Increased high-latitude photosynthetic carbon gain offset by respiration carbon loss during an anomalous warm winter to spring transition *Glob Change Biol* **26** 682–96
- López-Blanco E et al 2017 Exchange of CO<sub>2</sub> in Arctic tundra: impacts of meteorological variations and biological disturbance *Biogeosciences* **14** 4467–83
- Lund M et al 2010 Variability in exchange of CO<sub>2</sub> across 12 northern peatland and tundra sites *Glob Change Biol* **16** 2436–48
- Lund M et al 2012 Trends in CO<sub>2</sub> exchange in a high Arctic tundra heath, 2000–2010 *J. Geophys. Res.* **117** G02001
- Maes S L et al 2024 Environmental drivers of increased ecosystem respiration in a warming tundra *Nature* **629** 105–13
- Manzoni S, Chakrawal A, Fischer T, Schimel J P, Porporato A and Vico G 2020 Rainfall intensification increases the contribution of rewetting pulses to soil heterotrophic respiration *Biogeosciences* **17** 4007–23
- Merbold L et al 2009 Artificial drainage and associated carbon fluxes (CO<sub>2</sub>/CH<sub>4</sub>) in a tundra ecosystem *Glob Change Biol* **15** 2599–614
- Mertens S et al 2001 Influence of high temperature on end-of-season tundra CO<sub>2</sub> exchange *Ecosystems* **4** 226–36
- van der Molen M K et al 2007 The growing season greenhouse gas balance of a continental tundra site in the Indigirka lowlands, NE Siberia *Biogeosciences* **4** 985–1003
- Natali S M et al 2019 Large loss of CO<sub>2</sub> in winter observed across the northern permafrost region *Nat Clim Chang* **9** 852–7
- Oechel W C, Hastings S J, Vourlitis G, Jenkins M, Riechers G and Grulke N 1993 Recent change of Arctic tundra ecosystems from a net carbon dioxide sink to a source *Nature* **361** 520–3
- Oechel W C, Vourlitis G L, Hastings S J, Zulueta R C, Hinzman L and Kane D 2000 Acclimation of ecosystem CO<sub>2</sub> exchange in the Alaskan Arctic in response to decadal climate warming *Nature* **406** 978–81
- Ohta T, Kotani A, Iijima Y, Maximov T C, Ito S, Hanamura M, Kononov A V and Maximov A P 2014 Effects of waterlogging on water and carbon dioxide fluxes and environmental variables in a Siberian Larch forest, 1998–2011 *Agric. For. Meteorol.* **188** 64–75
- Panov A, Prokushkin A, Korets M, Putilin I, Zrazhevskaya G, Kolosov R and Bondar M 2024 Variation in soil CO<sub>2</sub> fluxes across land cover mosaic in typical tundra of the Taimyr peninsula, Siberia *Atmosphere* **15** 698
- Pearce R S 2001 Plant freezing and damage *Annals of Botany* **87** 417–24
- Post E et al 2009 Ecological dynamics across the Arctic associated with recent climate change *Science* **325** 1355–8
- Post E et al 2019 The polar regions in a 2 C warmer world *Sci. Adv.* **5** eaaw9883
- Post W et al 1982 Soil carbon pools and world life zones *Nature* **298** 156–9
- Rantanen M, Kämäräinen M, Luoto M and Aalto J 2024 Manifold increase in the spatial extent of heatwaves in the terrestrial Arctic *Commun. Earth Environ.* **5** 570
- Rantanen M, Karpechko A Y, Lipponen A, Nordling K, Hyvärinen O, Ruosteenoja K, Vihma T and Laaksonen A 2022 The Arctic has warmed nearly four times faster than the globe since 1979 *Commun. Earth Environ.* **3** 168
- Robinson S A 2022 Climate change and extreme events are changing the biology of Polar Regions *Glob. Change Biol.* **28** 5861–4
- Schädel C et al 2016 Potential carbon emissions dominated by carbon dioxide from thawed permafrost soils *Nat. Clim. Chang.* **6** 950–3
- Scharlemann J P, Tanner E V, Hiederer R and Kapos V 2014 Global soil carbon: understanding and managing the largest terrestrial carbon pool *Carbon Management* **5** 81–91
- Schuur E A G et al 2015 Climate change and the permafrost carbon feedback *Nature* **520** 171–9
- Schuur E A G et al 2022 Permafrost and climate change: carbon cycle feedbacks from the warming Arctic *Annu. Rev. Environ. Resour.* **47** 343–71
- Serreze M C et al 2000 Observational evidence of recent change in the northern high-latitude environment *Clim. Change* **46** 159–207
- Suni T et al 2003 Long-term measurements of surface fluxes above a Scots pine forest in Hyytiälä, southern Finland 1996–2001 *Boreal Environ. Res.* **8** 287–302
- Teskey R, Wertin T, Bauweraerts I, Amey M, McGuire M A and Steppe K 2015 Responses of tree species to heat waves and extreme heat events *Plant Cell Environ* **38** 1699–712
- Thum T, Aalto T, Laurila T, Aurela M, Kolari P and Hari P 2007 Parametrization of two photosynthesis models at the canopy scale in a northern boreal Scots pine forest *Tellus B Chem Phys Meteorol* **59** 874–90
- Torn M and Dengel S 2022 AmeriFlux FLUXNET-1F US-NGC NGEE Arctic council ver. 3-5 AmeriFlux AMP dataset doi: 10.17190/AMF/1902838
- Torn M and Dengel S 2023 AmeriFlux base US-NGC NGEE Arctic council Ver. 3-5 AmeriFlux AMP dataset doi: 10.17190/AMF/1634883
- Torn M S et al 2025 Large emissions of CO<sub>2</sub> and CH<sub>4</sub> due to active-layer warming in Arctic tundra *Nat. Commun.* **16** 124
- Treharne R, Bjerke J W, Tømmervik H and Phoenix G K 2020 Extreme event impacts on CO<sub>2</sub> fluxes across a range of high latitude, shrub-dominated ecosystems *Environ. Res. Lett.* **15** 104084
- TheAmeriFlux Network <https://ameriflux.lbl.gov/> (accessed on 23 March 2024)
- TheDataPortal Serving the FLUXNET Community <https://fluxnet.org/data/> (accessed on 15 March 2024)
- Vekuri H et al 2023 A widely-used eddy covariance gap-filling method creates systematic bias in carbon balance estimates *Sci. Rep.* **13** 1720
- Wutzler T, Lucas-Moffat A, Migliavacca M, Knauer J, Sickel K, Šigut L, Menzer O and Reichstein M 2018 Basic and extensible post-processing of eddy covariance flux data with REdDyProc *Biogeosciences* **15** 5015–30
- Zheleznova I V and Gushchina D Y 2023 Variability of extreme air temperatures and precipitation in different natural zones in late XX and early XXI centuries according to ERA5 reanalysis data *Izv Atmos Ocean Phys* **59** 479–88
- Zohner C M et al 2020 Late-spring frost risk between 1959 and 2017 decreased in North America but increased in Europe and Asia *Proc. Natl. Acad. Sci. U.S.A.* **117** 12192–200
- Zona D, Lipson D A, Richards J H, Phoenix G K, Liljedahl A K, Ueyama M, Sturtevant C S and Oechel W C 2014 Delayed responses of an Arctic ecosystem to an extreme summer: impacts on net ecosystem exchange and vegetation functioning *Biogeosciences* **11** 5877–88
- Zscheischler J, Reichstein M, Harmeling S, Rammig A, Tomelleri E and Mahecha M D 2014 Extreme events in gross primary production: a characterization across continents *Biogeosciences* **11** 2909–24